Research on Engineering Structures & Materials
www.jresm.org
Research Group

Research Article

Solar energy-driven heat treatment of concrete and mortar in desert environments: A case study of Bechar region, Algeria

Tidjar Boudjemaa [*1,2,a], Khelafi Hamid [3,b], Bella Nabil [1,c], Bennaceur Saïd [4,d], Lammari Khelifa [5,e], Benabdelfattah Mohamed [3,f], Hadj Djelloul Nasser Dine [1,g], Slimani Abdeldjalil[2,h], Dahbi Abdeldjalil [2,3,i]

[1]*FIMAS Laboratory, University of Tahri Mohammed, Bechar B.P 417, Bechar, 08000, Algeria*
[2]*Unité de Recherche en Energies Renouvelables en Milieu Saharien, URERMS, Centre de Développement des Energies Renouvelables, CDER, 01000, Adrar, Algeria*
[3]*Faculty of sciences and technologies, University of Adrar. Laboratory of Sustainable Development and Computer Science (LDDI), University of Adrar, Ahmed Draïa, RN6, 01000 Adrar, Algeria*
[4]*Laboratory for the Development of Renewable Energies and their Applications in Saharan Areas (LDREAS), Faculty of Exact Sciences, TAHRI Mohammed University, BP 417 Béchar, Algeria*
[5]*Faculty of Exact Sciences. Energy Laboratory in Arid Zones (ENERGARID). University of Béchar, TAHRI Mohammed, Algeria*

Article Info

Article History:

Received 07 Feb 2025
Accepted 17 June 2025

Keywords:

Early-age strength;
Concrete mass loss;
Total shrinkage;
Endogenous shrinkage;
Solar energy treatment;
Energy consumption

Abstract

This study investigates the effectiveness of solar energy-based heat treatment for concrete and mortar as a sustainable alternative to conventional curing methods. The approach aims to enhance early-age strength while reducing energy consumption, lowering production costs, and minimizing environmental impact. The acceleration of concrete and mortar hardening contributes to early-age strength development, which is beneficial for the prefabricated construction industry. Two treatment cycles were conducted: The first was: A 10 hours cycle in a solar dryer (SD) and an oven, reaching a maximum temperature of 55°C, with an average relative humidity of 60%. The second was: A 12 hours cycle in a solar greenhouse (SG), achieving 60°C with 50% relative humidity. The results of the tests were compared with those of the control specimens, hardened in at 25°C, 50% of relative humidity. The heat treatment significantly enhanced early-age strength development. On day one, mortar flexural strengths in SD, oven, and SG reached 25%, 25%, and 18%, respectively, of 28 days control specimen strength. However, treatment conditions did not significantly affect flexural strength at 120 days, with treated specimens exhibiting strengths comparable to control specimens. Moreover, these treatments lower concrete production costs while reducing CO_2 emissions by approximately 214.6 g/m^3, underscoring their positive environmental impact.

1. Introduction

Currently, the technological development that is happening in the world has led to a trend toward the use of renewable energy due to global warming gas emissions from conventional energy production [1]. Renewable energies are promising alternatives and without contributing to global warming gas emissions [2], their use is very important in various applications, providing a solution to growing energy consumption, while improving energy stability and sustainability [3].

*Corresponding author: boudjtidjar@yahoo.fr
[a]orcid.org/0000-0002-9915-4610; [b]orcid.org/0000-0002-3617-0437; [c]orcid.org/0000-0003-3586-8304; [d]orcid.org/0000-0001-7230-5792; [e]orcid.org/0000-0003-0679-5425; [f]orcid.org/0000-0003-4504-4560; [g]orcid.org/0000-0003-3296-7112; [h]orcid.org/0000-0002-8983-1702; [i]orcid.org/0000-0003-3630-6688
DOI: http://dx.doi.org/10.17515/resm2025-680en0207rs

Solar energy, earth's most abundant and perpetual resource, can be directly harnessed from solar radiation. The earth's surface receives approximately 100000 TW of solar energy annually [4]. Algeria's desert regions rank among the world's highest solar-exposed areas, averaging 10 hours of daily irradiation [5] and 2500–4000 hours annually [6]. This makes solar energy an efficient, sustainable solution for southern Algeria. Among these applications, heat treatment of cement products serves as a notable example [7], which also reduces energy costs in developing economies [8,9] .

Heat treatment accelerates cementitious materials hardening to achieve high early-age strength [10,11]. However, this treatment can negatively impact the long-term properties of the cement materials [12]. The durability of heat-treated cementitious materials is influenced by many factors, including the method of treatment [13].

A single heat treatment cycle suffices to achieve high demolding resistance in the short-term [14], final strength is typically attained during storage [15]. Heat treatment aims to accelerate early-age strength development through elevated temperatures. The American Concrete Institute (ACI) [16] and Zeyad et al. [17] recommend steam curing as the standard method, which typically follows a four-stage cycle:

- Preheating period: The temperature is maintained at or slightly above ambient levels for up to 4 hours [18].
- Heating period: The rate of temperature increase is substantially constant from 13 °C to 30 °C per hour [19,20].
- Isothermal period: The temperature is kept constant, Erdogˇdu et al. [21] and Türkel et al. [22] recommend the optimal temperatures treatment range from 60°C to 80°C.
- Cooling period: The temperature of the treated element returns to ambient temperature.

Several researchers Naas et al. [23] and Hanif et al. [24] have adopted the practice of using cooling rates equivalent to the rate of temperature increase during the heating period. Famy et al. [25] preferred the cooling speed to be slower than the heating speed. The sudden drop in temperature leads to cracks, which can compromise concrete strength. However, other researchers Yazici et al. [26] and Liu et al. [27] have adopted a cooling phase practice for a shorter period of the heating phase.

Rapid reheating of concrete above 70°C accelerates cement hydration, leading to late ettringite formation and potential sulfate attack [28]. While elevated temperatures enhance early-age strength through rapid CSH (calcium silicate hydrate) gel formation [29] and increased hydration product density [30], they may compromise long-term durability [31]. Notably, solar-powered heat treatment of concrete is more energy-efficient [32].

The adoption of solar energy for concrete heat treatment presents significant economic and environmental advantages. Conventional methods rely on carbon-intensive processes, exacerbating CO_2 emissions, whereas renewable energy integration aligns with sustainable development goals by reducing both emissions and production costs. Solar-treated concrete demonstrates improved mechanical performance, minimizing long-term strength deficiencies observed in traditional heat curing. For instance, Benammar et al. [33] reported a 77% strength increase at 28 days compared to control specimens. Despite these benefits, no comprehensive study has yet evaluated renewable energy-based heat treatment for its triple advantage: Simultaneous strength enhancement, emission reduction, and cost efficiency. Therefore, this paper reviews the potential of concrete and mortar heat treatment by solar energy as a technology capable of:

- Early-age strength development for industrial applications (prefabricated concrete [34]).
- Operational cost savings through reduced energy demand.
- CO_2 emission mitigation.

In this study, the effect of the treatment method on the mechanical properties of concrete has been studied as well as its environmental impact. Solar heat treatment of concrete and mortar is expected to achieve the desired goal of improving strength, contributing to environmental sustainability, and reducing carbon dioxide emissions.

2. Materials and Methods

This section outlines the materials used, temperature analysis in SD, oven, and SG, test methods, concrete and mortar mix design, specimen preparation, and testing procedures.

2.1. Materials and Characterization

2.1.1 Cement

This study used CEM II/A-L 42.5 N cement for mortar and concrete mixtures. Table 1 presents its chemical composition, while Tables 2 and 3 show its mechanical and physical, respectively.

Table 1. Chemical composition of cement (%)

Cement	SO_3	SiO_2	Al_2O_3	Fe_2O_3	CaO	MgO	K_2O	Na_2O	Cl
CEM II/A-L 42.5 N	1.59	18.86	4.51	2.56	65.20	2.33	0.64	0.33	0.005

Table 2. Mechanical characteristics of cement

Cement CEM II/A-L 42.5 N	2 days Compression (MPa)	7 days Compression (MPa)	28 days Compression (MPa)
	17.4	36.9	45.7

Table 3. Physical characteristics of cement

Cement CEM II/A-L 42.5 N	
Consistency (%)	31
Expansion (mm)	1
Absolute density (g/cm3)	3.10
Apparent density (g/cm3)	0.95
Fineness (cm2/g)	3750

2.1.2 Sand and Gravel

used rounded sand from Oued Ksiksou banks, with an apparent density of 1580 kg/m^3, specific density of 2600 kg/m^3, and fineness modulus 1.95, for all mortar and concrete mixtures. Locally produced crushed stones from Bechar region served as aggregates for concrete. Gravel 1 has an apparent density of 1430 kg/m^3 and specific density of 2620 kg/m^3, while gravel 2 has an apparent density of 1440 kg/m^3 and specific density of 2610 kg/m^3. The particle size curves of sand and gravel are given in Fig. 1.

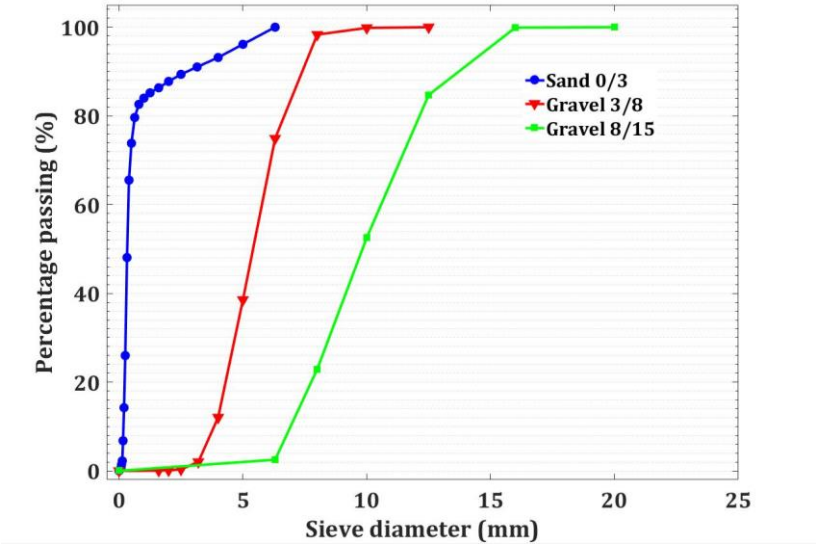

Fig. 1. The particle size distribution of sand and gravel

2.2. Mortar and Concrete Mix

The concrete mix comprised (0/3 mm) sand, (3/8 mm) gravel 1, and (8/15 mm) gravel 2. The desired workability is characterized by a subsidence to the cone of Abrams A=6.5 cm (plastic concrete). For the concrete formulation, we chose the Dreux-Gorisse method. This method makes it possible to determine the optimal quantities of the various components (sand, cement, gravel, water), based on particle size analysis [35]. The concrete formulation obtained is characterized by a water/cement ratio of 0.55, a sand percentage of 30%, gravel (3/8 mm) 34%, and gravel (8/15 mm) 36%. Mortar mixture proportions follow the EN 196-1 standard while maintaining the concrete's 0.55 W/C ratio to preserve the same cement matrix. The compositions of the concrete and mortar are presented in Table 4.

Table 4. Composition of concrete and mortar

Components	Water (kg/m^3)	Cement (kg/m^3)	W/C	Sand (kg/m^3)	Gravel 3/8 (kg/m^3)	Gravel 8/15 (kg/m^3)
Concrete	192.5	350	0.55	631.8	721.5	764
Mortar	247.5	450	0.55	1350	/	/

2.3. Heat Treatment Arrangement

A research team from the Laboratory of Energy in Arid Zones (ENERGARID) locally manufactured both SD and SG.

2.3.1 Sustainable Heat Treatment Systems

Operating partially through indirect solar energy via forced thermal convection, SD can also be powered entirely or partially by electricity. This dual capability allows it to function year-round, even in winter. However, SG, relies entirely on solar energy, limiting its nighttime use. Both models were constructed locally using raw materials purchased from ordinary markets in the Bechar region.

Fig. 2. The arrangement of the specimens. (a) in SD (b) in the greenhouse

Two systems were used for specimen drying. The first system, a SD, operates as an indirect thin-layer dryer using partial solar energy with forced convection (see Fig. 2a). This dryer also functions as an electric oven by covering the collector glass, blocking air inlet and outlet, and activating the electrical resistances in the heating unit. The second system is a fully solar-powered greenhouse (see Fig. 2b). We measured temperatures and humidity with a combined temperature-humidity sensor.

2.3.2 Specimens Preparation

We prepared the concrete and mortar at room temperature using the following procedure: Dry-mixed the aggregates and cement for one minute and 30 seconds to achieve homogeneity. Added two-thirds of the water and mixed for 2 minutes. Incorporated the remaining water and continued

mixing for 5 minutes (4 minutes for mortar). After mixing, we poured concrete into cubic molds (100 mm × 100 mm × 100 mm) and mortar into prismatic molds (40 mm × 40 mm × 160 mm). Each mold was filled in two layers and compacted on a vibrating table.

2.3.3 Solar Heat Treatment Cycles and Processing Protocol

Immediately after casting, all molds were covered with a plastic film, and the specimens were then subjected to heat treatment using solar energy. The placement of specimens in both SG and SD is illustrated in Fig. 3. Humidity is supplied in both systems by the air humidifier, as shown in Fig. 3b. The specimens were exposed to three different drying practical cycles the first and second in SD and oven for 10 hours, and the third for 12 hours in the SG, as shown in Fig. 4.

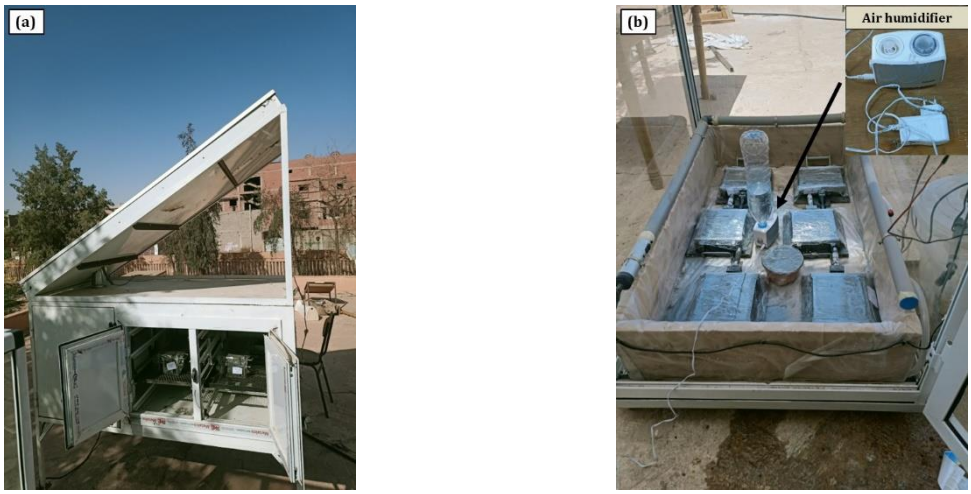

Fig. 3. Heat treatment system (solar radiation drying): (a) SD, (b) SG

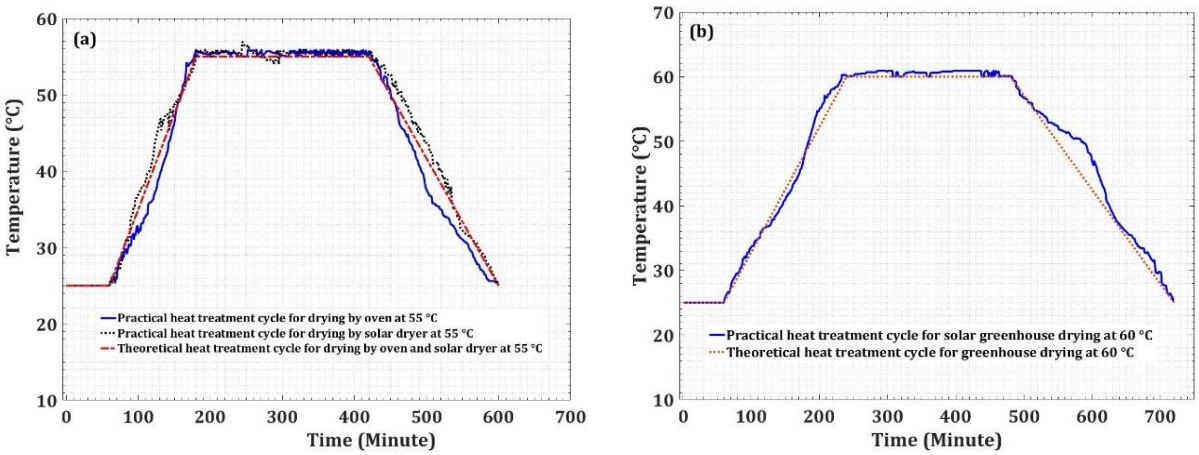

Fig. 4. Practical and theoretical heat treatment cycles for drying by (a) SD and oven; (b) SG

The processing cycle includes four phases:

- Preheating: Temperature remains constant at 25°C for one hour across all cycles.
- Heating: Temperature increases at 15°C/h for 2 hours in the first and second cycles, and at 11.6°C/h for 3 hours in the third cycle.
- Isothermal phase: Temperature maintains at 55°C for 4 hours in the first and second cycles, and at 60°C for 4 hours in the third cycle.
- Cooling: Temperature decreases to ambient levels at 15°C/h for 3 hours in the first and second cycles, and at 8.75°C/h for 4 hours in the third cycle.

2.4. Experimental investigation

We conducted an experimental program to study how different drying methods influence evaluation indicators, energy saving, and economic impact. We compared results with control specimens across three drying cycles: Oven, SD and SG.

2.4.1 Compressive Strength

The compressive strength test on concrete (100 mm × 100 mm × 100 mm) cubic specimens was conducted using a 300 KN capacity press, a continuous and regular load was applied at a constant rate of 1 mm/min until fracture. The maximum fracture force of the specimen was recorded (KN), with three specimens tested for each concrete mixture.

2.4.2 Flexural Strength

We determined flexural strength using (40 mm × 40 mm × 160 mm) prismatic specimens according to EN 196-1. The maximum (KN) at specimen fracture was recorded on the display screen. Data for each mortar represent average values from three tests.

2.4.3 Mass Loss Investigation

We measured mortar mass loss Pm(t) at the end of each cycle period, after demolding, and continuing through 120 days. The mass m(t) was measured by electronic balance with a relative uncertainty of ±0.2 g. We calculated specimen mass loss as follows:

$$Pm(t) = \frac{m(t) - m_0}{m_0} \quad (1)$$

Where, m_0: Mass of mould after pouring mortar before demolding or the mass of the specimen after demolding, m(t): Mass of the mould at the late of each cycle period before release or the mass of the specimen after t days after release. The mass loss value retained is the average of three measurements on (40 mm × 40 mm × 160 mm) test specimens.

2.4.4 Shrinkage Investigation Endogenous and Total

We conducted shrinkage tests on (40 mm × 40 mm × 160 mm) prismatic specimens. After treatment cycle and demolding, endogenous shrinkage specimens were covered with three layers: A first layer of cellophane plastic film and two additional layers of aluminum foil. This process is necessary to prevent external exchange and evaporation (see Fig. 5a). For shrinkage measurement, specimens (40 mm × 40 mm × 160 mm) were prepared following the standard NF P 15-433. These measurements were carried out using a linear variation comparator to determine the length change of the specimens (see Fig. 5b). Final reported shrinkage values represent averages from three specimens.

(a) (b)

Fig. 5. Shrinkage specimens and measurement device. (a) Endogenous shrinkage specimens; (b) Shrinkage measurement device

2.4.5 Energy Consumption

Energy consumed during the treatment cycle is measured using a wattmeter located in the control box mounted on the back face of the drying chamber, as shown in Fig. 6.

Fig. 6. Calculation of energy consumed

3. Results and Interpretations

3.1. Compressive Strength

The compressive strength test was carried out on cubic specimens (100 mm × 100 mm × 100 mm) immediately after the drying cycles up to 120 days.

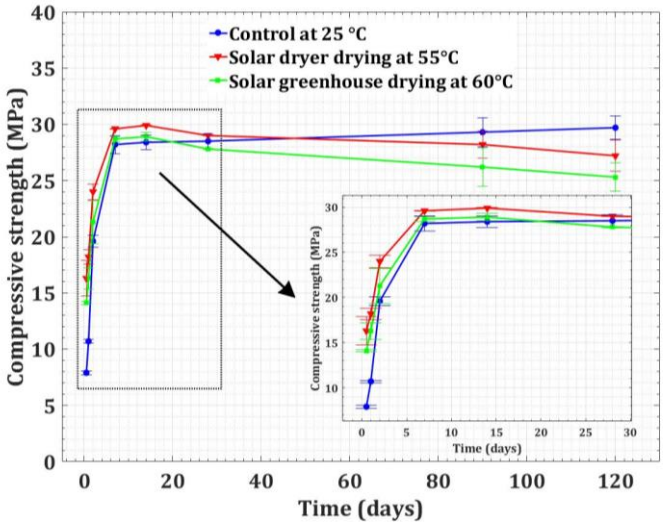

Fig. 7. Influence of the heat treatment method by solar energy on the development of compressive strength

3.1.1 Early-age Compressive Strength

As shown in Fig. 7, the control concrete exhibited a low compressive strength of 7.9 MPa after 12 hours of storage in the laboratory at 25°C, which was lower than the target strength of 10 MPa. In contrast, the SD and SG concretes exceeded 10 MPa, reaching 14.1 MPa and 16.3 MPa, respectively, after treatment. By the second day, their compressive strengths increased to 24 MPa for SD and 21.3 MPa for SG, representing 99.8% and 99.7%, respectively, of the 28 days strength of the control specimen. This improvement was attributed to the elevated temperature during both the final heating and isothermal phases, which accelerated hydration. This process promoted rapid formation of CSH [36], leading to increased material density [37,38] and, consequently, enhanced early-age compressive strength.

3.1.2 Medium-term Compressive Strength

The compressive strength of SG and SD treated specimens decreased after 28 days compared to the control specimens. This reduction was primarily attributable to less uniform distribution of hydration products in the paste, caused by initial rapid hydration [39]. These results align with findings from Benammar et al. [33], Emmanue et al. [40], and Benouadah et al. [41]. Additionally, concrete specimens treated in SD and SG showed a 1 MPa decrease in compressive strength at 28 days compared to 14 days. Moreover, at 28 and 90 days, their compressive strengths were slightly lower than those of the control specimens.

3.1.3 Long-Term Compressive Strength

At 120 days, SD and SG treated concrete reached a compressive strength of 27.2 MPa and 25.3 MPa, respectively, representing 99.92% and 99.85% of the control concrete strength. Furthermore, as expected, the increased humidity in SD during treatment yielded slightly greater long-term compressive strength compared to that of SG. This confirms Nabil et al. [42] conclusion that humidity enhances strength development during heating. In addition, both treated specimens exhibited slight strength reductions in the long-term. This phenomenon was attributed primarily to solar radiation exposure and elevated temperatures during the initial hardening phase. These conditions have accelerated the cement hydration process in the presence of free water within the concrete mixture, which is consistent with the conclusions of Mehdizadeh et al. [43].

3.2. Flexural Strength

The flexural strength tests were carried out on prismatic mortar specimens of dimensions (40 mm × 40 mm × 160 mm), using three specimens per test immediately after heating cycles at ages 12 hours, 1, 2, 7, 14, 28, 90, and 120 days. Fig. 8 illustrates the influence of method and temperature of heat treatment on the specimens treated by solar energy and the control specimens with respect to the development of flexural strength.

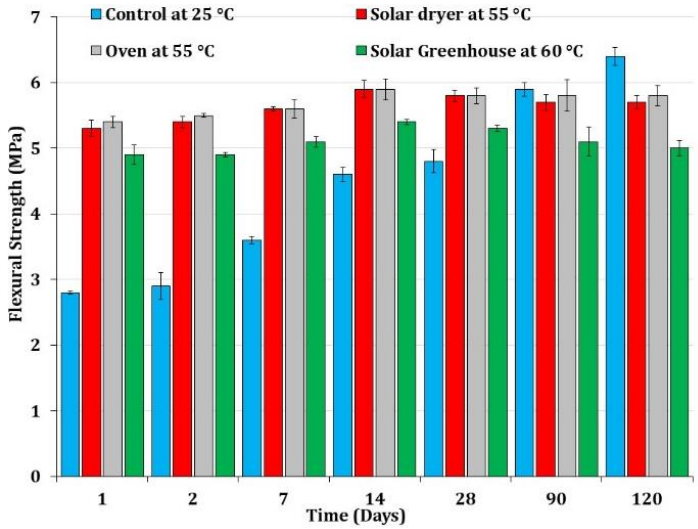

Fig. 8. Influence of the heat treatment method by solar energy on the development of flexural strength

3.2.1 Early-age Flexural Strength

The flexural strength results correlated closely with compressive strength development under all treatment conditions. The dryer and oven treated specimens demonstrated remarkably similar strength behavior, which was attributed to their identical treatment cycles. Testing confirmed that greenhouse, dryer, and oven treatments significantly improved early-age flexural strength development. At 24 hours, dryer and oven treated specimens achieved the highest flexural strengths 5.3 MPa, 5.4 MPa, respectively. This improvement results from air condensation (the greenhouse effect) and elevated temperatures, which accelerated cement hydration and produced greater early-age strength compared to control specimens and SG treated specimens.

3.2.2 Medium and Long-Term Flexural Strength

While the control specimens showed continued flexural strength gain, heat-treated specimens exhibited strength reduction after 14 days. This behavior was primarily attributed to rapid initial hydration, which resulted in less compact microstructural formation of hydration products [44].

3.3. Mass Loss

Fig. 9 shows mortar mass loss over time under different temperatures and heating methods. The mass loss trends of the different mortars are similar; it increases rapidly during the treatment cycle and tends to stabilize as the hardening age progresses.

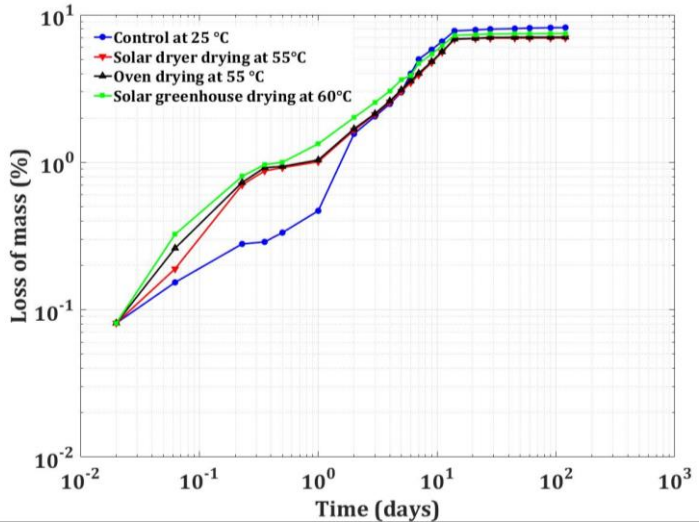

Fig. 9. Mass loss for the specimens treated and the control mortar

3.3.1 Initial Mass Loss

Oven, SD, and SG treated mortars showed the highest mass losses 0.92%, 0.94%, and 1% after 12 hours, respectively, while the control mortar lost only 0.33%. Parrott [45] and Jiang et al. [46] have demonstrated that free water evaporation causes mass loss. Studies have confirmed that higher initial free water content leads to greater mass loss [47]. After six days, control specimens demonstrated greater mass loss than treated specimens, as the latter had already lost significant water during treatment. SD, oven, and SG treated specimens showed more rapid initial mass loss and reached equilibrium faster than control specimens.

3.3.2 Stability of Mass Loss

Mass loss of the heat-treated specimens stabilized by day 14, reaching values of 6.81%, 6.84%, and 7.25%, respectively. However, the control specimen achieved mass loss stability later, at day 21, with 7.89%. This stabilization occurs when CSH gels form, filling pores and reducing water evaporation at later ages, which confirms the long-term flexural and compressive strength results.

3.4. Total Shrinkage of Mortar

3.4.1 First Phase: Increase of Total Shrinkage

Fig. 10 shows that on the first day, shrinkage values reached 154, 159, 173, and 81 μm/m for SD, oven, greenhouse treated, and control mortars, respectively. The SG treated specimen exhibited the highest shrinkage, which was attributable to elevated hardening temperatures combined with low relative humidity.

Following the rapid development phase, shrinkage values progressively increased to final measurements of 1009, 1027, 1081, and 579 μm/m for the respective specimens. All heat-treated mortars demonstrated continued shrinkage growth with age, with significantly more rapid development compared to the control specimen, which showed more gradual shrinkage progression. During the initial 60 days period for dryer and oven treated specimens and the first

35 days for SG specimens, total shrinkage showed comparable and significant deformation. These values were slightly higher than those measured in control specimens at 70 days.

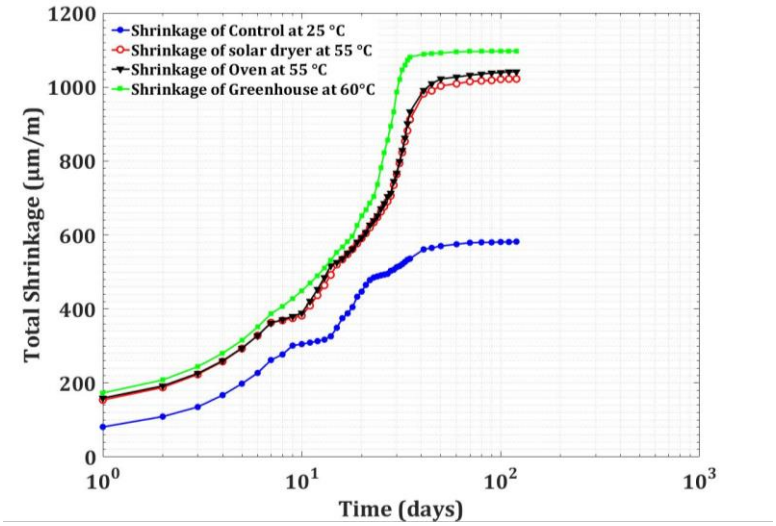

Fig. 10. Total shrinkage evolution for the specimens treated and the control mortar

Elevated hardening temperatures significantly increased shrinkage, this finding is consistent with the results of Bouziadi et al. [48], where higher temperatures accelerate hydration but create irregular CSH distribution, increasing early-age porosity and shrinkage [49,50]. This explains the rapid short-term shrinkage development in heat-treated specimens.

3.4.2 Second Phase: Stability of Total Shrinkage

In this phase, shrinkage tends to stabilize. After the initial setting and hardening phase, total specimen shrinkage reaches stability due to rapid water loss caused by high temperatures during treatment.

3.5. Endogenous Shrinkage of Mortar

Fig. 11 demonstrated rapid early-age endogenous shrinkage development across all mortar specimens, resulting from auto-desiccation of the cementitious matrix during hydration and hardening. The heat-treated specimens exhibited gradually decreasing shrinkage until day 21, while the control specimen showed continued reduction until day 35.

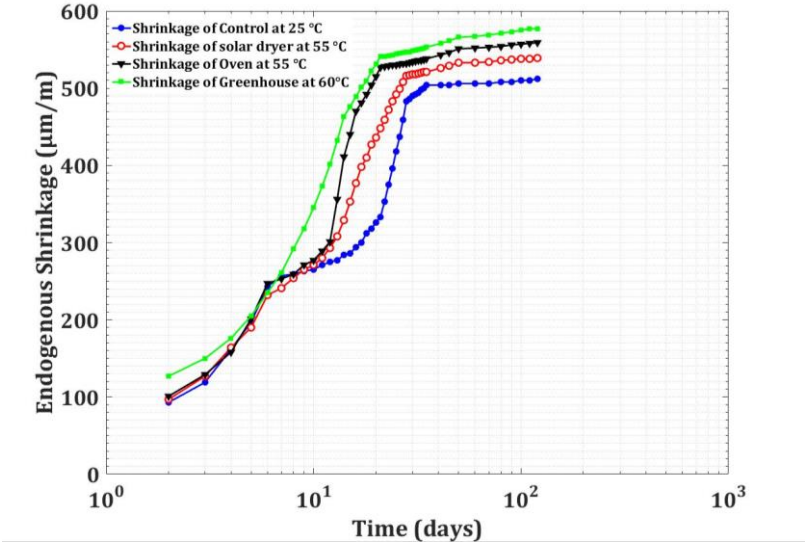

Fig. 11. Endogenous shrinkage evolution for the specimens treated and the control mortar

By 120 days, endogenous shrinkage values converged to 539 µm/m (SD), 559 µm/m (oven), 577 µm/m (SG), and 512 µm/m (control), despite differing treatment conditions.

3.6. Economic and Environmental Feasibility of the Study

3.6.1 Energy Consumption

Table 5 compares the energy consumption (E_c) during specimen treatment cycles between the partially electricity-powered SD and the oven using traditional heat treatment methods. Both specimens exceeded the desired compressive strength after the first day. The SD specimen, using renewable energy, achieved 16.3 MPa, surpassing the electric-powered oven specimen's value of 14.3 MPa. Furthermore, the oven consumed 0.79 kWh/m^3 of electrical energy, while the SD specimen, consumed 0.21 kWh/m^3.

Table 5. Electrical energy consumed

Heat treatment method	Renewable energy	Traditional method (electric power)
Energy consumed during the cycle (KWh)	0.35	1.36
Mass of specimens (Kg)	1.70	1.72
Energy to dry 1 m3 (KWh/m3)	0.21	0.79
Compressive strength after 24 hours (MPa)	16.3	14.3

As shown in Fig. 12, conventional heat treatment methods exhibited substantially higher energy requirements than renewable alternatives. The oven's energy consumption (0.79 kWh/m^3) was 3.8 times greater than SD, representing an estimated energy savings of 0.58 kWh/m^3 through solar drying. These energy savings contribute to reduced CO_2 emissions. According to the Intergovernmental Panel on Climate Change (IPCC) [51], producing 1 kWh of energy contributes to the emission of 370 g of CO_2. Consequently, using SD saves approximately 214.6 g of CO_2 emissions per 1 m^3 of concrete.

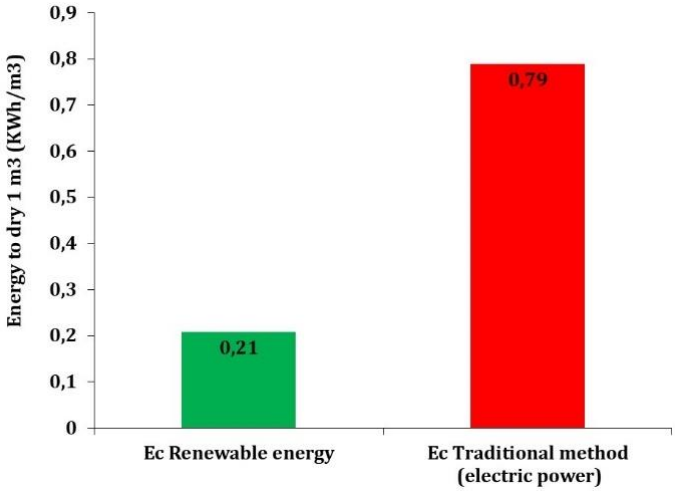

Fig. 12. Energy consumed by heat treatment

3.6.2 Environmental and Economic Impact

To evaluate environmental impact through CO_2 emissions and economic effectiveness, we conducted a financial analysis comparing conventional and renewable energy-based heating methods for mortar mixes. We applied the C_p indicator developed by Ma et al. [52]. The cost-efficiency and environmental impact C_p is calculated according to the following Eq (2):

$$C_p = \frac{Cost}{f_{c28}} \tag{2}$$

Where, Cost: Total material cost per cubic meter, f_{c28}: 28 days compressive strength. The costs of local raw materials in Algeria were taken from previous research by Benammar et al. [53], these values are detailed in Table 6.

Table 6. Cost of raw materials

Materials	Sand	Cement	Water	Energy	Heating
Real study Cost ($/kg) [53]	0.029	0.12	0.00372	($/kwh)	0.28

Fig. 13 shows the calculated C_p values for mortars treated with renewable energy versus electric energy. The C_p values of electrically treated mortar significantly exceed those of renewable energy treated mortar. The C_p values of conventionally treated mortar were approximately 4.4 times greater than those treated with renewable energy. This difference stems from the higher electricity costs compared to renewable energy sources, contributing to the increase C_p in electrically treated mortar.

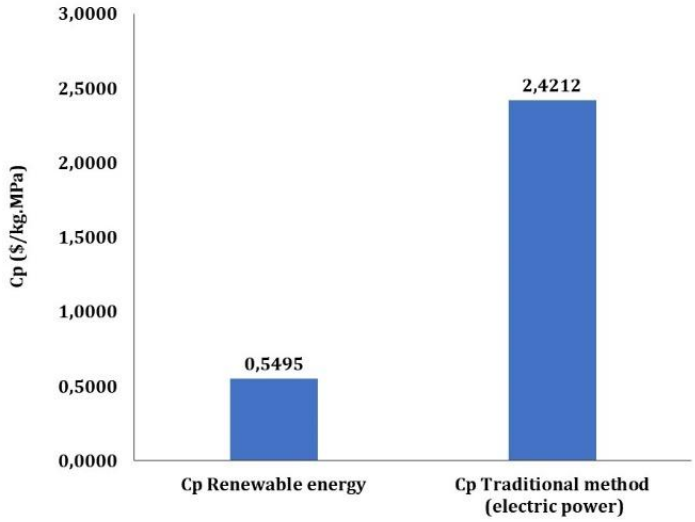

Fig. 13. The cost-efficiency and environmental impact

4. Effectiveness of the Study in the Global Context

This research demonstrates significant potential for global application, particularly in regions with abundant solar energy. The findings support solar heat treatment as a viable, cost-effective alternative to conventional treatment methods. Furthermore, our study supports previous similar research by Aruova et al. [54] and Sarkisov et al. [55] from other regions of the world, concluding that solar thermal treatment enhances early-age strength, provides an environmentally friendly approach, and offers cost-efficiency compared to traditional treatment methods.

The method's simplicity and scalability make it especially suitable for prefabricated construction in developing countries, where energy costs pose challenges. Additionally, its congruence with sustainable construction practices enhances its relevance worldwide, contributing to international efforts to reduce the environmental impact of concrete production. Further validation in diverse industrial settings could strengthen its global applicability. However, the study provides a strong foundation for adopting solar heat treatment as a practical, eco-friendly solution in the construction sector.

5. Conclusion

This study demonstrated the viability of solar heat treatment as a sustainable method for enhancing the early-age strength of concrete and mortar without compromising long-term performance. The results confirmed that this approach not only reduces production costs and energy consumption but also significantly lowers CO_2 emissions, supporting its potential for large-scale adoption in precast construction.

An experimental procedure evaluated the effect of the method of heat treatment of concrete and mortar by solar energy on the strength. Additionally, other properties such as mass loss, total

shrinkage, and endogenous shrinkage were studied. The results achieved were compared to control specimens.

Energy from SD, oven and SG accelerated hydration of cement paste, resulting in:

- Early-age strength enhancement: Treated specimens achieved rapid strength development, reaching 99.8% in SD and 99.7% in SG of 28 days control strength within two days. Notably, early-age rapid strength gain did not influence long-term strength.
- Mass loss: Heat-treated exhibited high mass loss compared to control specimens, mainly attributed to the evaporation of free water during treatment.
- Total shrinkage: Early-age shrinkage was similar between treated and control specimens. However, long-term shrinkage diverged, with treated specimens exhibiting higher values.
- Endogenous shrinkage: Consistency appeared between treated and control specimens in the short and long-term. However, the control specimens consistently exhibited higher endogenous shrinkage values than treated specimens.

Based on these results, the following conclusions can be drawn:

- The abundance of solar radiation in areas with the highest solar radiation in the world should be exploited in the concrete industry, which would allow savings in the industrial sector.
- Miniature models of SD and SG, represent a preliminary step toward developing of drying chambers for cement-based materials such as bricks, curbs, and decorative elements. This innovation benefits the economy by reducing energy consumption costs and contributes to environmental protection by lowering CO_2.
- Heat treatment by solar energy accelerates and increases the strengths of concrete and mortar in the short-term, without negatively affecting their long-term strengths.
- SD and oven yielded similar results, this similarity stems from comparable treatment cycles and the maximum temperature of the isothermal period at 55°C, these results are slightly higher than those in SG, where higher temperatures (60°C) and lower humidity reduced performance slightly.
- The utilization of solar energy, particularly through SD, reduced energy consumption by approximately 3.8 times for treating 1 m^3 of concrete, which has resulted in a reduction in carbon dioxide emissions, thus ensuring environmental preservation. Furthermore, the cost-effectiveness of heat treatment using renewable energy enhances environmental effectiveness by a factor of 4.4.

These results prove that treatment with renewable energies is a promising viable alternative to conventional heat treatment, enabling rapid strength gain while maintaining mechanical properties. This approach deserves consideration for implementation in construction applications, where rapid strength gain at an early-age is critical, particularly in geographic areas characterized by abundant solar radiation.

References

[1] Bahadori A, Nwaoha C. A review on solar energy utilisation in Australia. Renewable and Sustainable Energy Reviews 2013;18:1–5. https://doi.org/10.1016/j.rser.2012.10.003.
[2] Tsoutsos T, Frantzeskaki N, Gekas V. Environmental impacts from the solar energy technologies. Energy Policy 2005;33:289–96. https://doi.org/10.1016/S0301-4215(03)00241-6.
[3] Madlool NA, Saidur R, Hossain MS, Rahim NA. A critical review on energy use and savings in the cement industries. Renewable and Sustainable Energy Reviews 2011;15:2042–60. https://doi.org/10.1016/J.RSER.2011.01.005.
[4] Bhutto AW, Bazmi AA, Zahedi G. Greener energy: Issues and challenges for Pakistan-Solar energy prospective. Renewable and Sustainable Energy Reviews 2012;16:2762–80. https://doi.org/10.1016/j.rser.2012.02.043.
[5] Gairaa K, Khellaf A, Benkacilai S, Guermoui M. Solar radiation measurements in Algeria: case of Ghardaïa station as member of the enerMENA meteorological network. Energy Procedia 2017;141:50–4. https://doi.org/10.1016/j.egypro.2017.11.010.
[6] Boukar M, Harmim A. Performance evaluation of a one-sided vertical solar still tested in the Desert of Algeria. Desalination 2005;183:113–26. https://doi.org/10.1016/j.desal.2005.02.045.

[7] Pirasteh G, Saidur R, Rahman SMA, Rahim NA. A review on development of solar drying applications. Renewable and Sustainable Energy Reviews 2014;31:133–48. https://doi.org/10.1016/J.RSER.2013.11.052.
[8] Mahn D, Best R, Wang C, Abiona O. What drives solar energy adoption in developing countries? Evidence from household surveys across countries. Energy Econ 2024;138:107815. https://doi.org/10.1016/j.eneco.2024.107815.
[9] Opoku R, Adjei EA, Ahadzie DK, Agyarko KA. Energy efficiency, solar energy and cost saving opportunities in public tertiary institutions in developing countries: The case of KNUST, Ghana. Alexandria Engineering Journal 2020;59:417–28. https://doi.org/10.1016/j.aej.2020.01.011.
[10] Bella IA, Asroun A, Bella N. Effect of Curing Temperature on Mortar Based on Sustainable Concrete Material's and Poly-Carboxylate Superplasticizer. Journal of Civil Engineering and Architecture 2014;8:66. https://doi.org/10.17265/1934-7359/2014.01.008.
[11] Shi J, Liu B, He Z, Wu X, Tan J, Chen J, et al. Properties evolution of high-early-strength cement paste and interfacial transition zone during steam curing process. Constr Build Mater 2020;252:119095. https://doi.org/10.1016/j.conbuildmat.2020.119095.
[12] Gonzalez-Corominas A, Etxeberria M, Poon CS. Influence of steam curing on the pore structures and mechanical properties of fly-ash high performance concrete prepared with recycled aggregates. Cem Concr Compos 2016;71:77–84. https://doi.org/10.1016/j.cemconcomp.2016.05.010.
[13] Ranz J, Aparicio S, Fuente J V., Anaya JJ, Hernández MG. Monitoring of the curing process in precast concrete slabs: An experimental study. Constr Build Mater 2016;122:406–16. https://doi.org/10.1016/j.conbuildmat.2016.06.041.
[14] Baoju L, Youjun X, Shiqiong Z, Jian L. Some factors affecting early compressive strength of steam-curing concrete with ultrafine fly ash. Cem Concr Res 2001;31:1455–8. https://doi.org/10.1016/S0008-8846(01)00559-2.
[15] He Z, Liu J, Zhu K. Influence of mineral admixtures on the short and long-term performance of steam-cured concrete. Energy Procedia 2011;16:836–41. https://doi.org/10.1016/j.egypro.2012.01.134.
[16] Committee ACI. Cementitious Materials for Concrete. ACI Education Bulletin E3-13 ACI Committee E-701(2013) ACI Education Bulletin E3-13 Cementitious Materials for Concrete Recuperado 2013;15:950–5.
[17] Zeyad AM, Tayeh BA, Adesina A, de Azevedo ARG, Amin M, Hadzima-Nyarko M, et al. Review on effect of steam curing on behavior of concrete. Cleaner Materials 2022;3:100042. https://doi.org/10.1016/j.clema.2022.100042.
[18] Etxeberria M. The suitability of concrete using recycled aggregates (RAs) for high-performance concrete. Elsevier Ltd.; 2020. https://doi.org/10.1016/B978-0-12-819055-5.00013-9.
[19] Yang J, Hu H, He X, Su Y, Wang Y, Tan H, et al. Effect of steam curing on compressive strength and microstructure of high volume ultrafine fly ash cement mortar. Constr Build Mater 2021;266:120894. https://doi.org/10.1016/j.conbuildmat.2020.120894.
[20] Bi L, Long G, Ma C, Xie Y. Experimental investigation on the influence of phase change materials on properties and pore structure of steam-cured mortar. Archives of Civil and Mechanical Engineering 2021;21:1–10. https://doi.org/10.1007/s43452-020-00170-7.
[21] Erdoğdu S, Kurbetci S. Optimum heat treatment cycle for cements of different type and composition. Cem Concr Res 1998;28:1595–604. https://doi.org/10.1016/S0008-8846(98)00134-3.
[22] Türkel S, Alabas V. The effect of excessive steam curing on Portland composite cement concrete. Cem Concr Res 2005;35:405–11. https://doi.org/10.1016/j.cemconres.2004.07.038.
[23] Naas A, Taha-Hocine D, Salim G, Michèle Q. Combined effect of powdered dune sand and steam-curing using solar energy on concrete characteristics. Constr Build Mater 2022;322. https://doi.org/10.1016/j.conbuildmat.2022.126474.
[24] Hanif A, Kim Y, Usman M, Park C. Optimization of steam-curing regime for recycled aggregate concrete incorporating high early strength cement-a parametric study. Materials 2018;11. https://doi.org/10.3390/ma11122487.
[25] Famy C, Scrivener KL, Atkinson A, Brough AR. Influence of the storage conditions on the dimensional changes of heat-cured mortars. Cem Concr Res 2001;31:795–803. https://doi.org/10.1016/S0008-8846(01)00480-X.
[26] Yazici H, Aydin S, Yiğiter H, Baradan B. Effect of steam curing on class C high-volume fly ash concrete mixtures. Cem Concr Res 2005;35:1122–7. https://doi.org/10.1016/j.cemconres.2004.08.011.
[27] Liu B, Xie Y, Li J. Influence of steam curing on the compressive strength of concrete containing supplementary cementing materials. Cem Concr Res 2005;35:994–8. https://doi.org/10.1016/j.cemconres.2004.05.044.
[28] Amine Y, Leklou N, Amiri O. Effect of supplementary cementitious materials (scm) on delayed ettringite formation in heat-cured concretes. Energy Procedia 2017;139:565–70. https://doi.org/10.1016/j.egypro.2017.11.254.

[29] Li W, Fan Y, Hong J, Shi Y, Yang D, Wang P. Investigation on the early proceeding of cement hydration containing dispersed nano Calcium Silicate Hydrated (CSH) seeds. Constr Build Mater 2024;425:136039. https://doi.org/10.1016/j.conbuildmat.2024.136039.
[30] Shi J, Liu B, Zhou F, Shen S, Guo A, Xie Y. Effect of steam curing regimes on temperature and humidity gradient, permeability and microstructure of concrete. Constr Build Mater 2021;281:122562. https://doi.org/10.1016/j.conbuildmat.2021.122562.
[31] Ramezanianpour AA, Khazali MH, Vosoughi P. Effect of steam curing cycles on strength and durability of SCC: A case study in precast concrete. Constr Build Mater 2013;49:807–13. https://doi.org/10.1016/j.conbuildmat.2013.08.040.
[32] Yu K, Jia M, Yang Y, Liu Y. A clean strategy of concrete curing in cold climate: Solar thermal energy storage based on phase change material. Appl Energy 2023;331:120375. https://doi.org/10.1016/j.apenergy.2022.120375.
[33] Benammar B, Mezghiche B, Guettala S. Influence of atmospheric steam curing by solar energy on the compressive and flexural strength of concretes. Constr Build Mater 2013;49:511–8. https://doi.org/10.1016/j.conbuildmat.2013.08.085.
[34] Sebaibi N, Boutouil M. Reducing energy consumption of prefabricated building elements and lowering the environmental impact of concrete. Eng Struct 2020;213:110594. https://doi.org/10.1016/j.engstruct.2020.110594.
[35] Hamza C, Bouchra S, Mostapha B, Mohamed B. Formulation of ordinary concrete using the dreux-gorisse method. Procedia Structural Integrity 2020;28:430–9. https://doi.org/10.1016/j.prostr.2020.10.050.
[36] He J, Long G, Ma K, Xie Y. Comprehensive study on the hydration kinetics, mechanical properties and autogenous shrinkage of cement pastes during steam curing. Cem Concr Res 2023;174:107310. https://doi.org/10.1016/j.cemconres.2023.107310.
[37] Balaji T, Jeyashree TM, R KRP, J BS. Effect of elevated temperature on concrete incorporating zeolite , silica fume and fly ash as replacement for cement 2024;x:1–14. https://doi.org/10.17515/resm2024.267ma0506rs.
[38] Gallucci E, Zhang X, Scrivener KL. Effect of temperature on the microstructure of calcium silicate hydrate (C-S-H). Cem Concr Res 2013;53:185–95. https://doi.org/10.1016/j.cemconres.2013.06.008.
[39] John E, Lothenbach B. Cement hydration mechanisms through time – a review. J Mater Sci 2023;58:9805–33. https://doi.org/10.1007/s10853-023-08651-9.
[40] Emmanuel AC, Krishnan S, Bishnoi S. Influence of curing temperature on hydration and microstructural development of ordinary Portland cement. Constr Build Mater 2022;329:127070. https://doi.org/10.1016/j.conbuildmat.2022.127070.
[41] Benouadah A, Merbouh M, Nabil B, Benammar A. Effect of Self-Curing Admixture and Sand Type on the Mechanical and Microstructural Properties of Concrete in Hot Climate Conditions. Annales de Chimie. Science des Materiaux, vol. 48, International Information and Engineering Technology Association (IIETA); 2024, p. 85. https://doi.org/10.18280/acsm.480110.
[42] Nabil B, Aissa A, Aguida BI. Use of a new approach (design of experiments method) to study different procedures to avoid plastic shrinkage cracking of concrete in hot climates. Journal of Advanced Concrete Technology 2011;9:149–57. https://doi.org/10.3151/jact.9.149.
[43] Mehdizadeh H, Jia X, Mo KH, Ling T-C. Effect of water-to-cement ratio induced hydration on the accelerated carbonation of cement pastes. Environmental Pollution 2021;280:116914. https://doi.org/10.1016/j.envpol.2021.116914.
[44] Bogner A, Link J, Baum M, Mahlbacher M, Gil-Diaz T, Lützenkirchen J, et al. Early hydration and microstructure formation of Portland cement paste studied by oscillation rheology, isothermal calorimetry, 1H NMR relaxometry, conductance and SAXS. Cem Concr Res 2020;130:105977. https://doi.org/10.1016/j.cemconres.2020.105977.
[45] Parrott LJ. Basic creep, drying creep and shrinkage of a mature cement paste after a heat cycle. Cem Concr Res 1977;7:597–604. https://doi.org/10.1016/0008-8846(77)90121-1.
[46] Jiang C, Jin C, Wang Y, Yan S, Chen D. Effect of heat curing treatment on the drying shrinkage behavior and microstructure characteristics of mortar incorporating different content ground granulated blast-furnace slag. Constr Build Mater 2018;186:379–87. https://doi.org/10.1016/j.conbuildmat.2018.07.079.
[47] Rebai K, Bella IA, Bella N, Seghir A. Contribution to the modeling of the short-term behavior of cured concrete in hot weather. Advances in Concrete Construction 2025;19:163–72. https://doi.org/10.12989/acc.2025.19.3.163.
[48] Bouziadi F, Boulekbache B, Hamrat M. The effects of fibres on the shrinkage of high-strength concrete under various curing temperatures. Constr Build Mater 2016;114:40–8. https://doi.org/10.1016/j.conbuildmat.2016.03.164.
[49] Jennings HM, Thomas JJ, Gevrenov JS, Constantinides G, Ulm FJ. A multi-technique investigation of the nanoporosity of cement paste. Cem Concr Res 2007;37:329–36. https://doi.org/10.1016/j.cemconres.2006.03.021

[50] Toledo Filho RD, Ghavami K, Sanjuán MA, England GL. Free, restrained and drying shrinkage of cement mortar composites reinforced with vegetable fibres. Cem Concr Compos 2005;27:537–46. https://doi.org/10.1016/j.cemconcomp.2004.09.005.
[51] Intergovernmental Panel on Climate Change. Technology-specific Cost and Performance Parameters. Climate Change 2014: Mitigation of Climate Change 2015:1329–56. https://doi.org/10.1017/cbo9781107415416.025.
[52] Ma C, Long G, Shi Y, Xie Y. Preparation of cleaner one-part geopolymer by investigating different types of commercial sodium metasilicate in China. J Clean Prod 2018;201:636–47. https://doi.org/10.1016/j.jclepro.2018.08.060.
[53] Benammar A, Noui A, Benouadah A, Maafi N, Kessal O, Dridi M, et al. Enhancing sustainability and performance in alkali-activated mortars with recycled rubber aggregates subjected to varied curing methods. Research on Engineering Structures and Materials 2024. https://doi.org/10.17515/resm2024.192ma0226rs.
[54] Aruova L, Shashpan Z h., Utkelbaeva A, Alibekov N. Solar Energy for Foam Concrete Production Technology in Modern Conditions. J Mech Eng Res Dev 2018;41. https://doi.org/10.26480/jmerd.02.2018.49.55.
[55] Sarkisov DA, Zhadanovskii B V, Sinenko SA, Esenov MK. Prospects for the use of solar energy to accelerate the hardening of concrete in the construction of monolithic structures in Russia. E3S Web of Conferences, vol. 284, EDP Sciences; 2021, p. 6001.